

Minimum semi-major axis of extrasolar planets in relation to dust sublimation zones

Frane Lunić

Supervisor: assoc.prof.dr. Dejan Vinković

Split, September 2014

Bachelor Thesis in Physics

Department of Physics
Faculty of Science
University of Split



Abstract

We studied the relation of the present-day semi-major axis of extrasolar planets to dust sublimation zones at the time of formation of planets. We have used the NASA Exoplanet Archive to find the data on semi-major axes of planets and stellar masses. The masses were used for finding the appropriate models of stellar evolution in order to obtain the luminosities at different ages during the early phase of the evolution. The luminosities were then used to calculate the inner radii dividing the dusty disk from the sublimation zones and the inner dust free zone. The fractions of planets orbiting closer than each of the inner radii was then calculated.

The fractions varied from outermost to the innermost inner radii, but those of the innermost inner radii were at most ages small enough to support the in situ theory of formation of planets. In general, the fractions decreased with age in the considered interval. A cut-off in the density of distribution of planets was found near the innermost inner radius at the age of 2 Myr. The results seem to be compatible with the in situ theories of planet formation, but do not exclude alternative theories.

Acknowledgements

This research has made use of the NASA Exoplanet Archive, which is operated by the California Institute of Technology, under contract with the National Aeronautics and Space Administration under the Exoplanet Exploration Program.

Contents

1	Introduction	1
1.1	Background	1
1.2	Hypothesis	1
2	Methods	3
3	Results	4
4	Discussion	11
5	Conclusion	16
A	Python scripts	17
	Bibliography	23

List of Figures

3.1	Semi-major axis of Kepler Candidates and inner radii at 1 Myr with respect to stellar mass.	5
3.2	Semi-major axis of confirmed planets and inner radii at 1 Myr with respect to stellar mass.	6
3.3	Semi-major axis of Kepler Candidates and inner radii at 2 Myr with respect to stellar mass.	6
3.4	Semi-major axis of confirmed planets and inner radii at 2 Myr with respect to stellar mass.	7
3.5	Semi-major axis of Kepler Candidates and inner radii at 3 Myr with respect to stellar mass.	7
3.6	Semi-major axis of confirmed planets and inner radii at 3 Myr with respect to stellar mass.	8
3.7	Semi-major axis of Kepler Candidates and inner radii at 4 Myr with respect to stellar mass.	8
3.8	Semi-major axis of confirmed planets and inner radii at 4 Myr with respect to stellar mass.	9
3.9	Semi-major axis of Kepler Candidates and inner radii at 5 Myr with respect to stellar mass.	9
3.10	Semi-major axis of confirmed planets and inner radii at 5 Myr with respect to stellar mass.	10
4.1	Disk fraction (Ribas et al., 2014) and fractions of outliers with respect to age	12
4.2	Number of planets with respect to semi-major axis (scaled by division by luminosity of the host star) at age 1 Myr	13
4.3	Number of planets with respect to semi-major axis (scaled by division by luminosity of the host star) at age 2 Myr	14
4.4	Number of planets with respect to semi-major axis (scaled by division by luminosity of the host star) at age 3 Myr	14
4.5	Number of planets with respect to semi-major axis (scaled by division by luminosity of the host star) at age 4 Myr	15
4.6	Number of planets with respect to semi-major axis (scaled by division by luminosity of the host star) at age 5 Myr	15

Chapter 1

Introduction

1.1 Background

Planets that do not belong to the Solar System are called extrasolar planets. The study of other planetary systems provides the information useful for testing, among other, the theories of planet formation and planetary system evolution.

There are various methods of detection of extrasolar planets. The transit method works by measuring changes in the brightness of a star as a planet crosses in front of it. The Kepler Mission uses data produced by NASA's space observatory Kepler to detect transits and find potential extrasolar planets. This method is considered to produce a relatively high number of false positives and confirmation by other methods is required. However, the number of false positives for multi-planet systems may be low (Rowe et al., 2014). Another method is measuring variations in radial velocity of a star caused by the star orbiting around the system's shared center of mass. The variation is obtained from the displacement in spectral lines of a star due to Doppler effect.

According to the accepted theory of planet formation, this occurs by accretion of dust found in protoplanetary disks surrounding newly formed stars (Armitage, 2007). However, dust can not survive arbitrarily close to the star since it will become heated past its sublimation point, creating an inner disk hole composed of gas. For this reason planet formation might not be possible closer than a certain radius. But the transition from a dust containing disk to a region devoid of dust need not be sudden. A region containing only large dust grains would be optically thinner, and thus more capable of cooling itself by radiation. This would allow for the existence of a vast sublimation zone, containing only large grains of dust, in which planets may still form. (Vinković, 2006).

The aim of this thesis is to study the semi-major axis of detected extrasolar planets in relation to these sublimation zones. Knowing if the proposed existence of these zones affects the present position of planets could potentially present an important observational constraint for theories of planet formation and migration.

1.2 Hypothesis

Lacking solid material, planets should not be able to form closer to the star than R_{in} , the radius of the inner edge of the optically thin sublimation zone (further referred to as the "inner radius", assuming the inner radius of the optically thin disk unless stated otherwise). Supposing their orbits have not changed since the beginning of their formation, we would not expect to discover extrasolar planets orbiting at distances smaller than R_{in} .

If such planets are found, this discrepancy will have to be accounted for in theories of planetary system evolution. Discovery of planets at distances smaller than R_{in} would constitute indirect evidence for widespread occurrence of planetary migration, thought to occur due to interaction of forming planets with gas in the disk.

The hypothesis tested here states that planets were formed in situ¹, and should be farther away than the inner radius, except for those whose small semi-major axis may be explained away by some other process that we do not consider here.

¹Understood here as in the same or reasonably close orbit to where they are now.

Chapter 2

Methods

We have searched the cumulative list of Kepler Objects of Interest (KOIs) and the list of confirmed planets from the NASA Exoplanet Archive¹. Many entries were missing crucial data such as semi-major axis, stellar temperature and stellar mass, and were removed from the sample. To avoid working with known false positives and counting the confirmed planets twice, only KOIs dispositioned as "Candidate" were kept. Additionally conditions were imposed on temperature of the host star and number of planets orbiting a host. Host star temperature was required to fall in range between 3000 K and 10000 K, and number of planets to be greater than 1. From the remaining planets only those whose orbits had the smallest semi-major axes in their respective planetary systems were chosen. The final sample was comprised of 253 objects from the confirmed planets list (out of 1743) and 142 objects from the list of KOIs (out of 7305).

The aim was to compare the observed semi-major axes with the inner radii of the optically thin and thick disks at the time of formation of planets. The inner radii were calculated using the formula given in Vinković (2006):

$$R_{in} = 0.0344\psi \left(\frac{1500 \text{ K}}{T_{sub}} \right)^2 \sqrt{\frac{L_*}{L_\odot}} \quad [\text{AU}] \quad (2.1)$$

Here L_* and L_\odot are the stellar and the solar luminosity respectively, T_{sub} the sublimation temperature, and the parameter ψ represents the effects of the optical depth. ψ is set to 2 for optically thick disks, and 1.2 for optically thin disks (Vinković, 2006). The luminosities were estimated based on stellar time evolution models (Dotter et al., 2007). For each host star two most appropriate models were chosen based on the mass of the star (unless the model for that exact mass could be found) and the final result was obtained by linear interpolation between them. Multiple points in evolution between the ages of 1 Myr and 5 Myr were considered, and each time the results were interpolated in the same manner as with masses. Finally, for each combination of parameters ψ , T_{sub} and age, the fraction of the planets closer than the inner radius (further referred to as the "outliers") was calculated.

The process explained in this chapter was accomplished using two Python scripts specifically written for this purpose (available in the appendix A). The data was exported from the archive in .csv format, and was then searched, filtered and saved into another .csv file by running "filter.py". The rest of the process was completed by repeatedly running "plot.py" and changing the age parameter each time. The final results are given in chapter 3, and in chapter 4 an interpretation is given, taking into account the observational data on evolution of protoplanetary disks.

¹<http://exoplanetarchive.ipac.caltech.edu/index.html>

Chapter 3

Results

The results are presented here in form of scatter plots where each dot represents a confirmed planet or a candidate (only the planets nearest to their host star are presented). The horizontal axis represents stellar mass, and the vertical axis represents semi-major axis of planetary orbit. Four curves are drawn on each graph, representing the inner radii for different combinations of values of ψ and T_{sub} parameters at a given age, i.e. point in the evolution of stars.

For all combinations of ψ , T_{sub} and age parameters, fractions of planets with semi-major axis smaller than the inner radii, i.e. lying below the respective curve on the graph, are given in table 3.1.

Table 3.1: Numbers (NO) and fractions (FO) of outliers, given the age, ψ and T_{sub} parameters, compared with estimates of disk fractions based on the model given in Ribas et al. (2014)

Age [Myr]	ψ	T_{sub} [K]	Confirmed Planets		Kepler Candidates		All		Disk Fraction [%] (Ribas et al., 2014)
			NO	FO	NO	FO	NO	FO	
1	2	1500	153	60.47%	107	75.35%	260	65.82%	56 ± 8
	2	2000	67	26.48%	60	42.25%	127	32.15%	
	1.2	1500	75	29.64%	66	46.48%	141	35.70%	
	1.2	2000	13	5.14%	23	16.20%	36	9.11%	
2	2	1500	122	48.22%	94	66.20%	216	54.68%	38 ± 6
	2	2000	32	12.65%	40	28.17%	72	18.23%	
	1.2	1500	37	14.62%	44	30.99%	81	20.51%	
	1.2	2000	3	1.19%	12	8.45%	15	3.80%	
3	2	1500	99	39.13%	74	52.11%	173	43.80%	26 ± 4
	2	2000	20	7.91%	30	21.13%	50	12.66%	
	1.2	1500	23	9.09%	35	24.65%	58	14.68%	
	1.2	2000	2	0.79%	9	6.34%	11	2.78%	
4	2	1500	78	30.83%	67	47.18%	145	36.71%	18 ± 3
	2	2000	15	5.93%	24	16.90%	39	9.87%	
	1.2	1500	18	7.11%	28	19.72%	46	11.65%	
	1.2	2000	2	0.79%	6	4.23%	8	2.03%	
5	2	1500	69	27.27%	63	44.37%	132	33.42%	13 ± 2
	2	2000	11	4.35%	24	16.90%	35	8.86%	
	1.2	1500	14	5.53%	25	17.61%	39	9.87%	
	1.2	2000	1	0.40%	6	4.23%	7	1.77%	

As can be seen from figures 3.1 - 3.10 and table 3.1, in range between 0.5 and 1.5 solar masses, where most of the object's hosts are, the inner radii increase with age from 1 Myr to 5 Myr, and consequently, the percentages of outliers drop.

Generally, the outlier fractions of Kepler Candidates are greater than those of confirmed planets. A considerable fraction of objects are closer to the host star than the farthest inner radius ($\psi = 2$, $T_{sub} = 1500\text{K}$) at each point in evolution considered, from around a quarter at 5 Myr for confirmed planets up to around 60% at 1 Myr (three quarters for candidates). However, only a small fraction of objects are closer than the closest inner radius, down to only 1 confirmed planet (out of 253) at 5 Myr. These results are discussed in the following chapter.

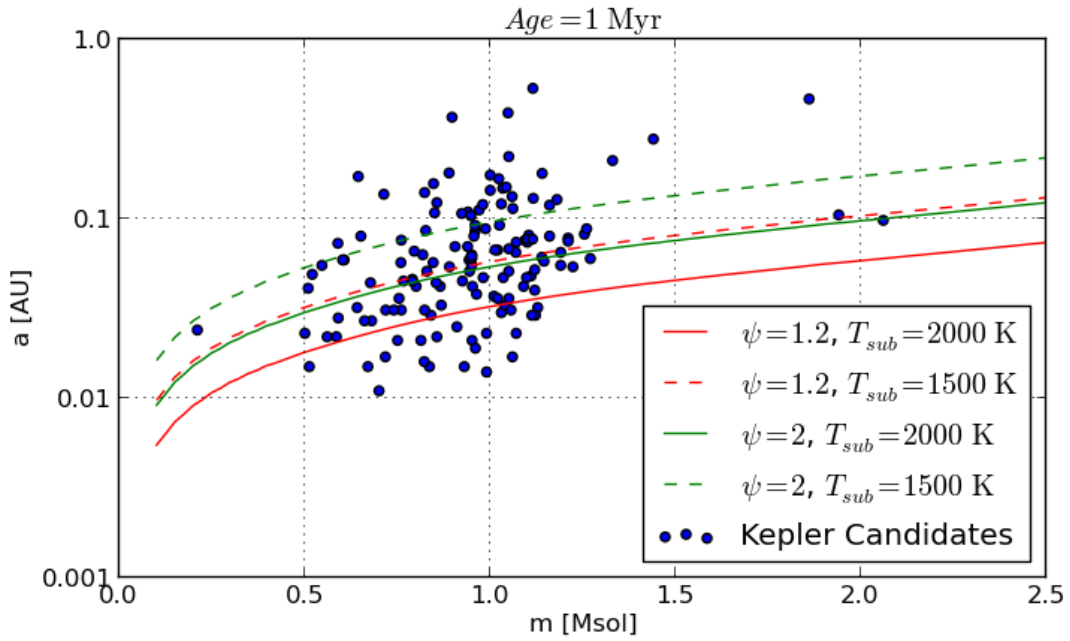


Figure 3.1: Semi-major axis of Kepler Candidates and inner radii at 1 Myr with respect to stellar mass.

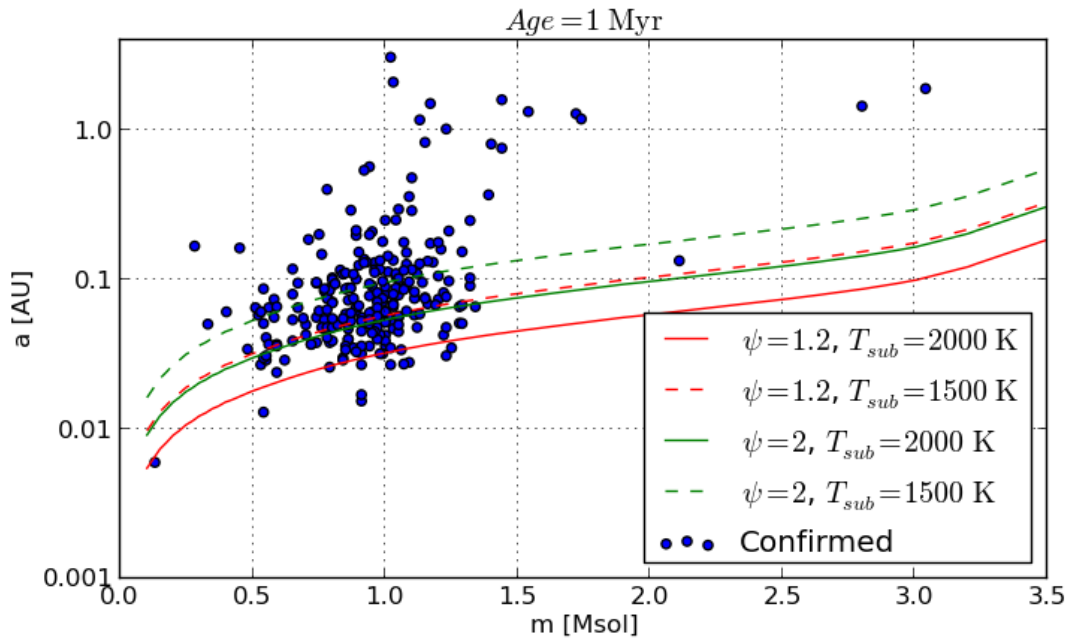


Figure 3.2: Semi-major axis of confirmed planets and inner radii at 1 Myr with respect to stellar mass.

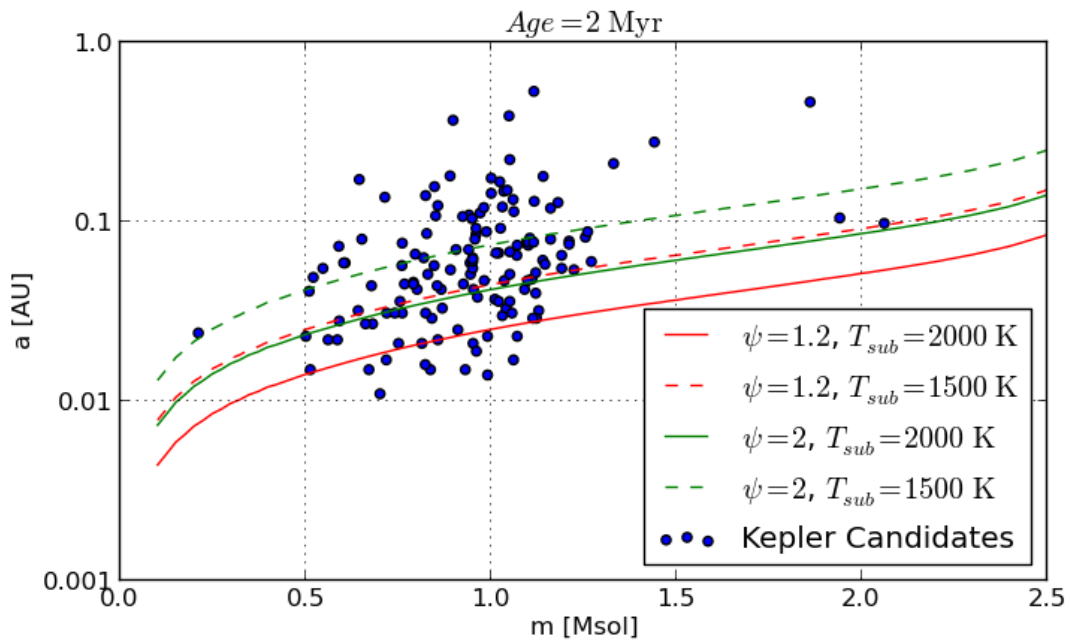


Figure 3.3: Semi-major axis of Kepler Candidates and inner radii at 2 Myr with respect to stellar mass.

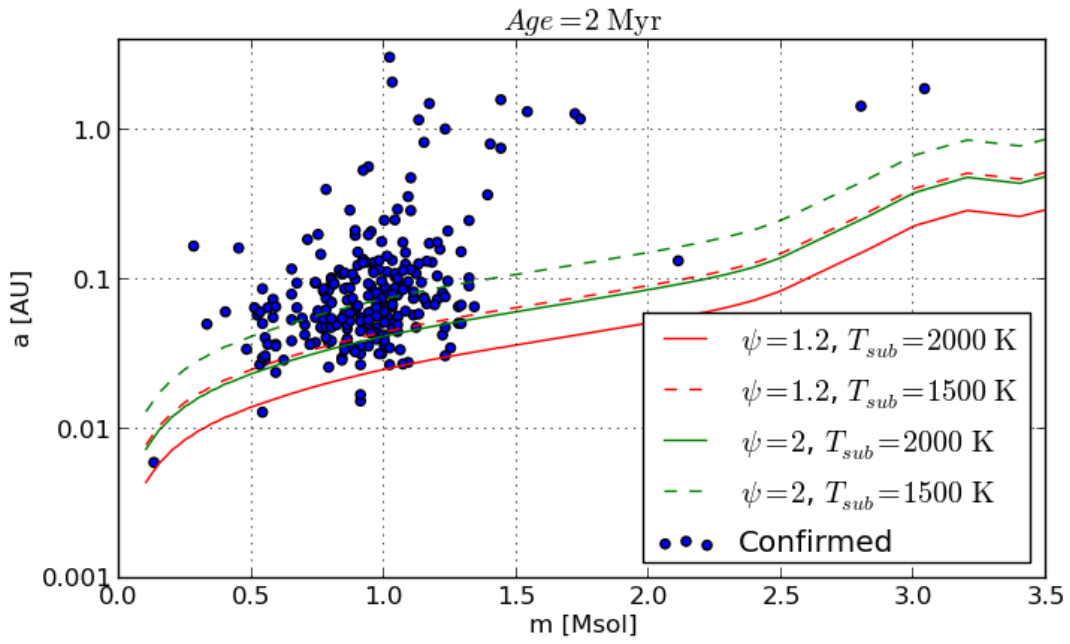


Figure 3.4: Semi-major axis of confirmed planets and inner radii at 2 Myr with respect to stellar mass.

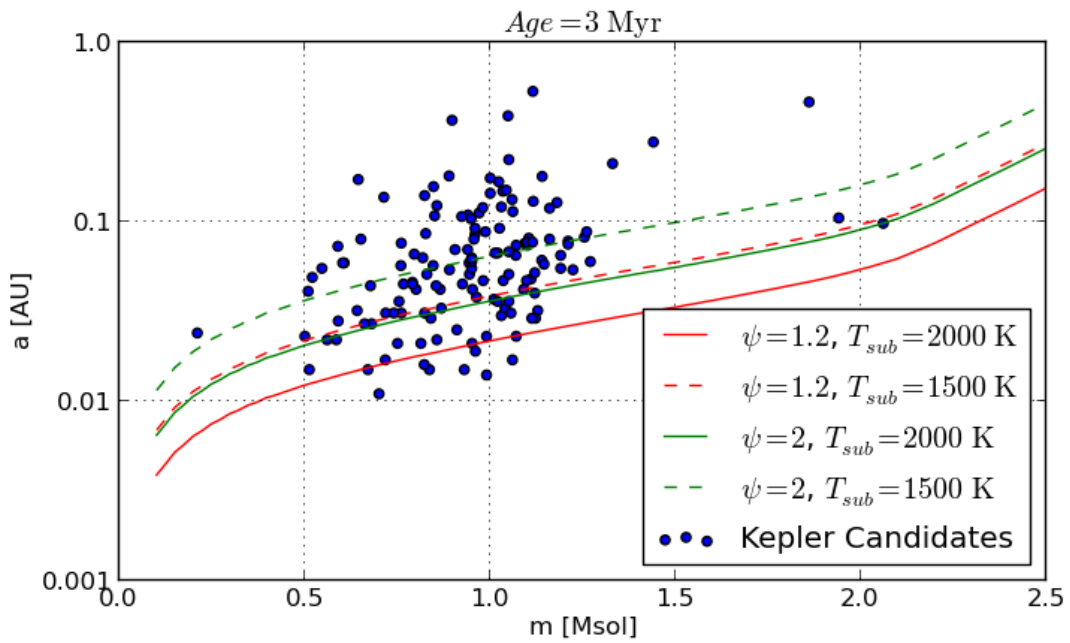


Figure 3.5: Semi-major axis of Kepler Candidates and inner radii at 3 Myr with respect to stellar mass.

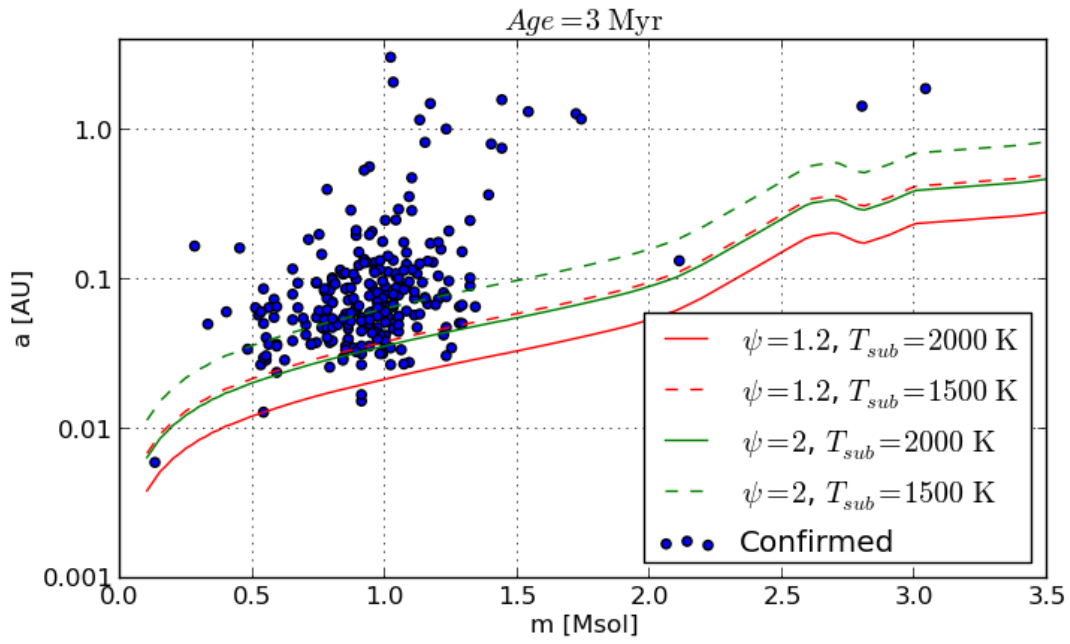


Figure 3.6: Semi-major axis of confirmed planets and inner radii at 3 Myr with respect to stellar mass.

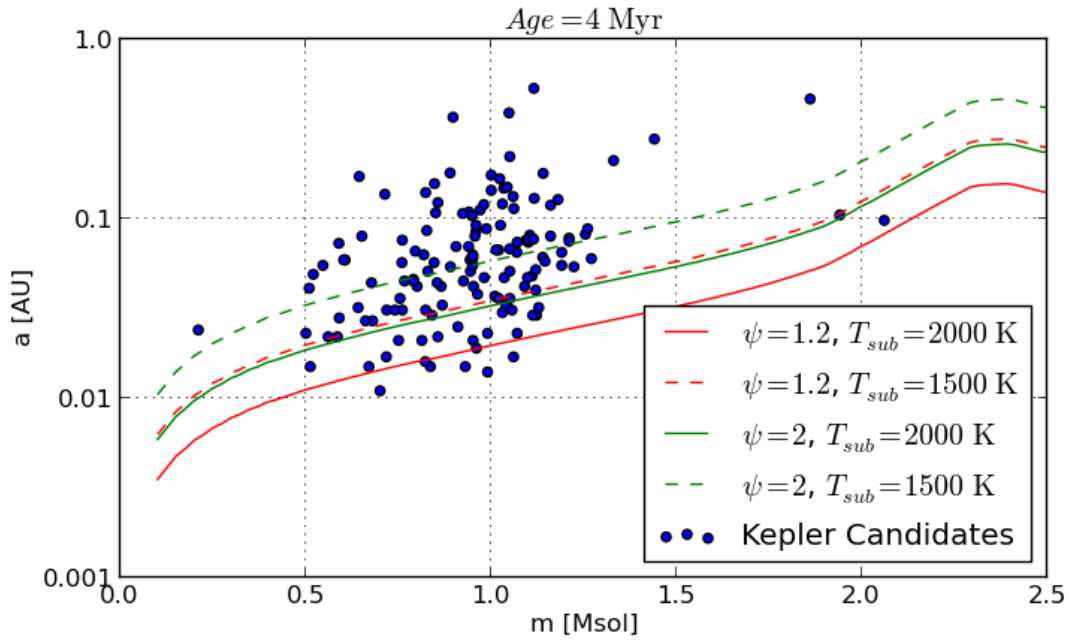


Figure 3.7: Semi-major axis of Kepler Candidates and inner radii at 4 Myr with respect to stellar mass.

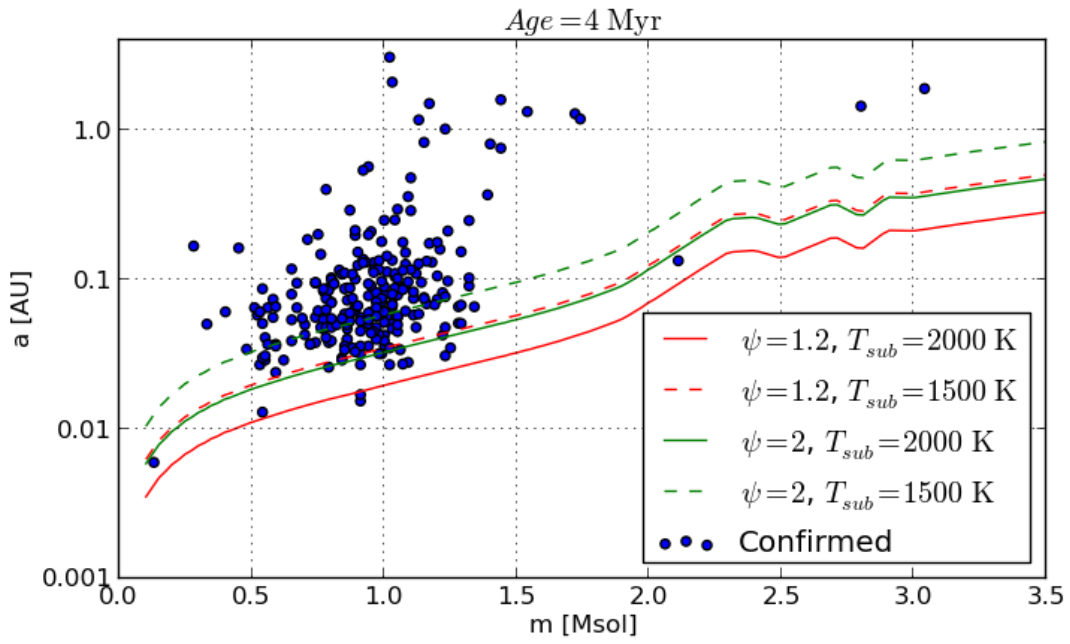


Figure 3.8: Semi-major axis of confirmed planets and inner radii at 4 Myr with respect to stellar mass.

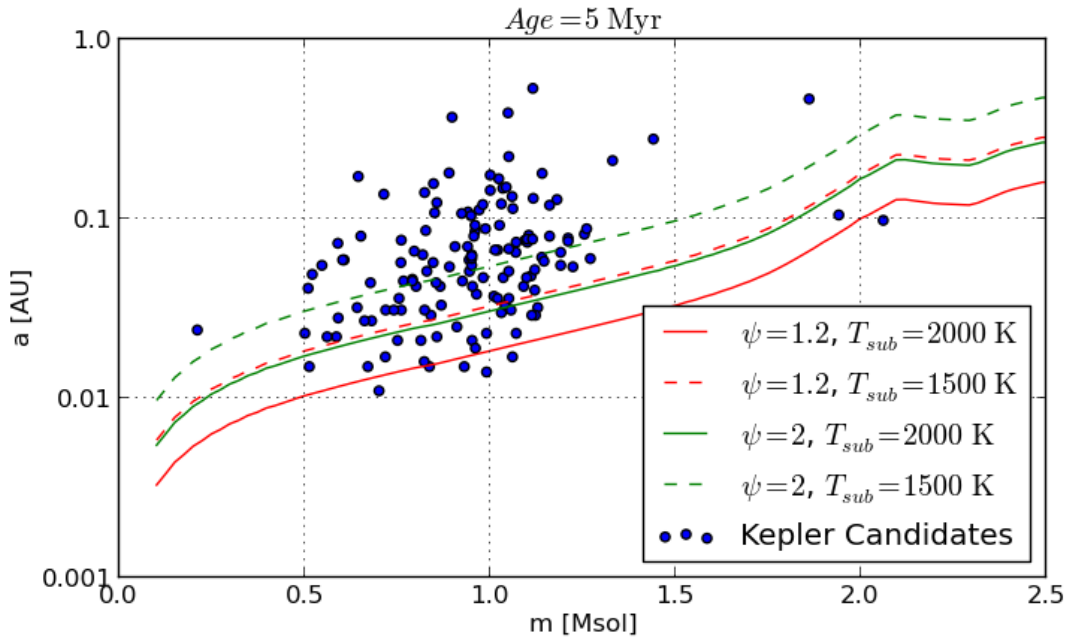


Figure 3.9: Semi-major axis of Kepler Candidates and inner radii at 5 Myr with respect to stellar mass.

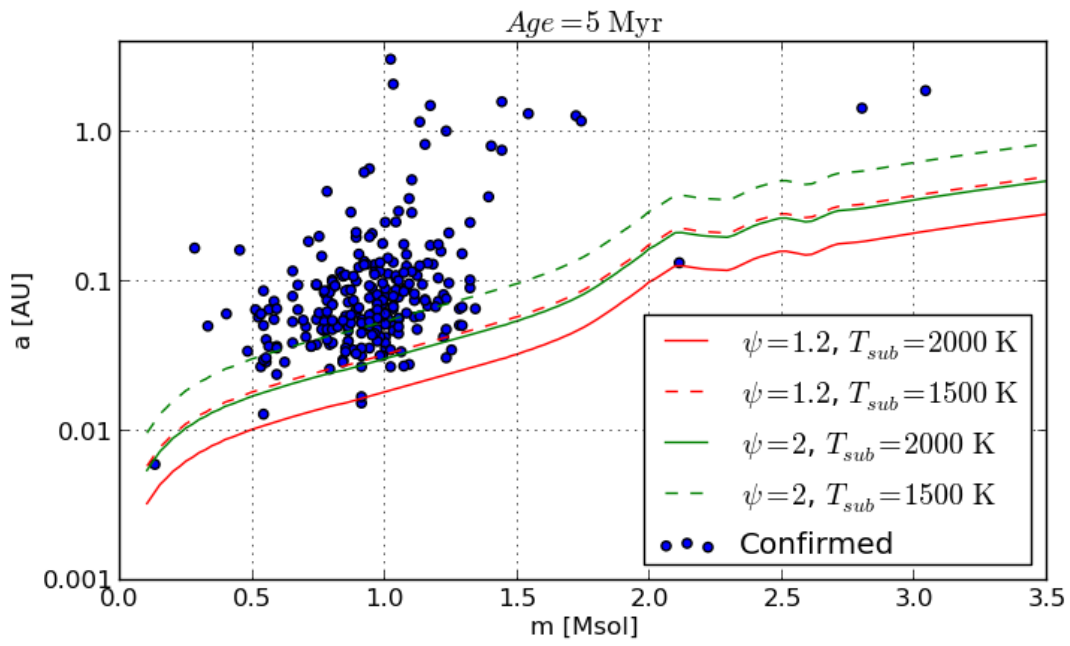


Figure 3.10: Semi-major axis of confirmed planets and inner radii at 5 Myr with respect to stellar mass.

Chapter 4

Discussion

Since most of the detected objects were removed from the sample (see chapter 2), caution is advised because the results could have been affected by small sample size, and biases can potentially arise from removal of objects if missing entries are correlated to some of the properties, e.g. semi-major axis.

As stated in the previous chapter, a large fraction of objects (at least a quarter) are closer than the farthest inner radius. This radius represents the sublimation point of optically thick dust composed of silicates ($T_{sub} = 1500$ K). Presumably, the mass surface density of dust drops after this point, but this does not necessarily prevent planet formation, meaning that this finding does not invalidate the hypothesis.

Between the closest and the furthest inner radii, there is the inner radius of optically thick dust composed of iron grains and the one of optically thin dust composed of silicates. Fractions of outliers for these radii are comparable, the fraction of the latter being slightly greater in general. These fractions, while being considerable at 1 Myr¹, drop below 10% at 3 Myr for confirmed planets. For candidates, however, they remain above 20% at 3 Myr and above 15% even at 5 Myr. From figure 3.6 one can see that the distribution of dots seems to become on average less dense below the two lines representing these radii for confirmed planets (note that usage of log scale is partly responsible for this appearance) This could be the result of a sudden drop in surface density of dust at these two inner radii. However, from the way dots are distributed², other reasons, beyond the scope of this thesis, may be suspected. Besides, this phenomenon is not as noticeable with candidates on figure 3.5.

Planets should not be detected closer than the inner radius of optically thin iron dust at time of formation unless the migration toward the host star happened during the evolution. As visible in table 3.1, there are planets orbiting closer than this radius at every considered age. However, for confirmed planets this fraction drops to only around 1% (three planets) at 2 Myr, and continues dropping to only one planet at 5 Myr. A quick glance at figure 3.10 shows that this planet orbits very close to the inner radius. Since the measured semi-major axes of planets and the parameters of the inner radius are approximate, it is possible that in reality the fraction of outliers at 5 Myr is zero³. The same reasoning applies for all ages and real fractions of outliers could be smaller (or greater) than the ones obtained here. Since the fractions of outliers are small it can not be excluded that these planets may have migrated here by some anomalous processes, leaving the hypothesis intact. As before, the fractions of outliers are greater for candidates, over 16% at 1 Myr, and they fall to around 8% at 2 Myr, and then continue falling less sharply to below 5% at 4 Myr. The same explanations as with confirmed planets may still be employed here, but larger fractions of outliers make them less powerful. Since these detections by Kepler have not been confirmed by other methods, some of them might turn out to be false positives, though, as mentioned in section 1.1, most of them are likely to be real planets. It is plausible that there

¹A bit less than 30% for confirmed planets, almost a half for candidates

²Notice how the drop in density seems to occur at a horizontal line instead of following an inner radius line

³Indeed, a small change of the parameters, e.g. $\psi = 1.15$ and $T_{sub} = 2050$ K, makes the planet's semi-major axis greater than the inner radius.

may be more false positives among the objects closer than the inner radius than in general, but this is questionable and other explanations should not be excluded.

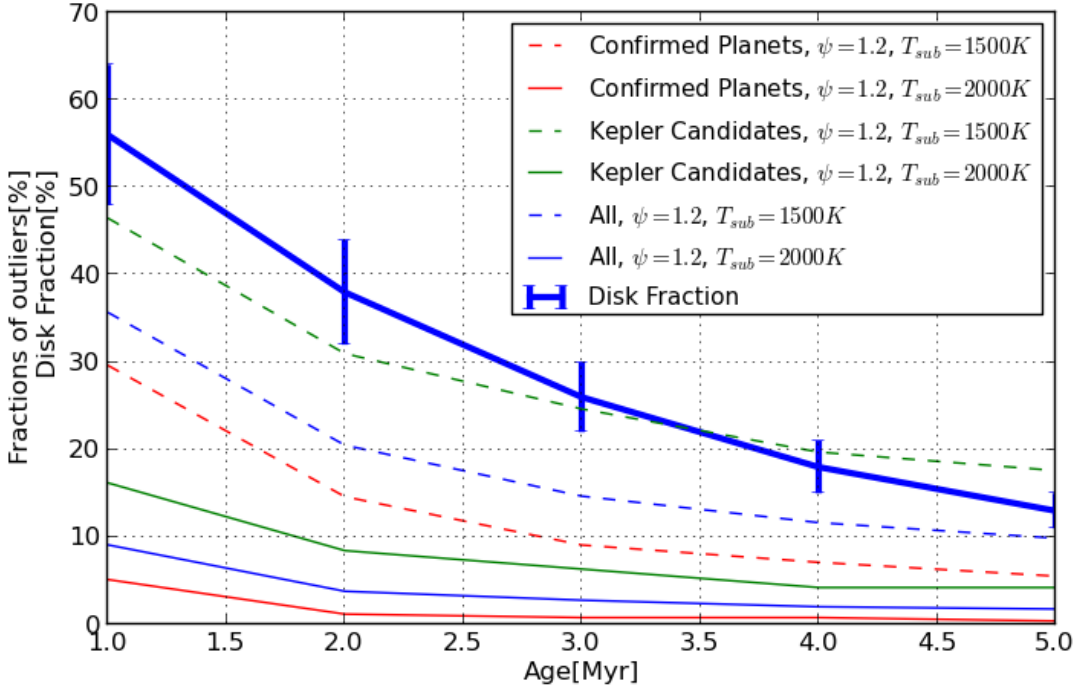


Figure 4.1: Disk fraction (Ribas et al., 2014) and fractions of outliers with respect to age

It is obvious from discussion so far that fractions of outliers at later ages are more supportive of the hypothesis, but for this discussion to be meaningful, the evolution of protoplanetary disks must be taken into account. Circumstellar disks can be detected by measuring the excess over the stellar radiation at different wavelengths in the infrared part of the spectrum, created by the disks. These excesses are studied in Ribas et al. (2014) and the ratios of sources displaying an excess over the total number of sources (referred to as "disk fractions") are calculated for different associations of young stars of known age. Based on calculated disk fractions, a best fit exponential model for evolution of disk fractions is derived. These disk fractions can be used to track the evolution of protoplanetary disks. Since the hot dust, near the sublimation zones radiates at shorter wavelengths than the dust farther away from the star it makes sense to use disk fractions obtained at these wavelengths (labeled "short" in Ribas et al. (2014)). The estimates of disk fractions are given in table 3.1 for each of the considered points in the evolution. The time evolution of disk fractions, along with those of fractions of outliers, is shown on figure 4.1.

Since planets are formed in protoplanetary disks, a small disk fraction implies that a majority of planets in the sample have already started their formation at a given age. By contrast, a large disk fraction would mean it is possible that a considerable number of the planets detected have not yet started their formation at that time. Planets detected closer than the inner radius may thus have started their formation at a later time, when their semi-major axis was greater than the inner radius. However, there is no reason to expect these yet-to-form planets should be clustered close to the star, so it is assumed that they will be distributed over a wide range of distances (following some general distribution of planets). But in case the fraction of outliers is much lower than the disk fraction, i.e. their ratio is small, the ongoing planet formation may explain their position. Another heuristic for deciding whether or not to consider this explanation plausible would be to compare the relative rates at which the fraction of outliers and the disk fraction drop. If the disk fraction drops faster than the fraction of outliers, then

at later ages the fraction of planet producing systems might be too small to account for the remaining outliers, meaning that other explanations should probably be sought.

At 1 Myr, the disk fraction ($\sim 56\%$) can be considered high enough to explain (combined with other factors discussed) the fraction of outliers since the ratio of the fraction of outliers to the disk fraction is not very large and becomes even smaller later on. However, the fraction of outlying candidates (16.2%) is much higher and thus harder to explain. Since the percentage of outlying candidates drops faster than the disk fraction between 1 Myr and 2 Myr, the ratio drops from ~ 0.3 to ~ 0.2 , its lowest point, and tends to rise afterwards. It seems that a considerable part of candidates closer than the inner radius at 3 Myr (6.34%) can not be explained in this manner, but due to small sample size, this result is likely not significant. Combined, Kepler Candidates and confirmed planets make a somewhat more formidable sample. The fractions of outliers now fall in between those of confirmed planets, and candidates. Since the sample size of confirmed planets is greater than that of candidates, and the number of outlying confirmed planets is insignificant already at 2 Myr, the combined sample turns out to be easily reconcilable with the hypothesis. The ratio, beginning at ~ 0.16 drops to ~ 0.1 at 2 Myr, stagnates, and then rises after 4 Myr. This (along with the evolution of disk fraction) suggests that most of the planet formation probably happened around 2 Myr, and very little went on after 4 Myr. Because the values of combined fractions of outliers between those two ages are of questionable significance, the hypothesis has not been invalidated, but the possibility of an alternative should not be excluded⁴

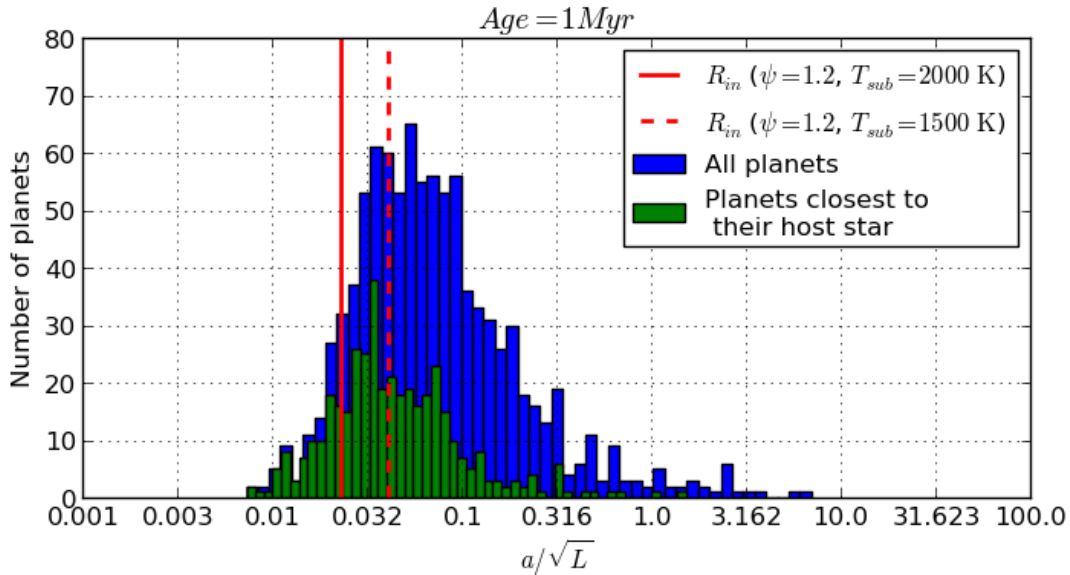


Figure 4.2: Number of planets with respect to semi-major axis (scaled by division by luminosity of the host star) at age 1 Myr

Another way to check if the inner radii influence the properties of planetary systems is to see how the distribution of planets changes with distance from the host star. If the hypothesis is true, we would expect to see some clustering of planets (especially those nearest to their host star) near the inner radius, and then a sharp drop in numbers. On figures 4.2 - 4.6, histograms of distance from the host star are shown. To compare the distances of planets in different systems, the distances have to be scaled, i.e. divided, by $\sqrt{L_*}$ (as discussed in Vinković and Jurkić, 2007). This process eliminates the dependence of inner radii and other characteristic distances on the luminosity of the star. Evidence of the expected

⁴Since the mass density of dust drops between the inner radii for 1500 K and 2000 K, as points of sublimation of various substances are encountered, the best inner radius to perform an analysis on could be somewhere between these two. The fractions of outliers would be greater, but this is beyond the scope of this thesis, since this is only a preliminary analysis

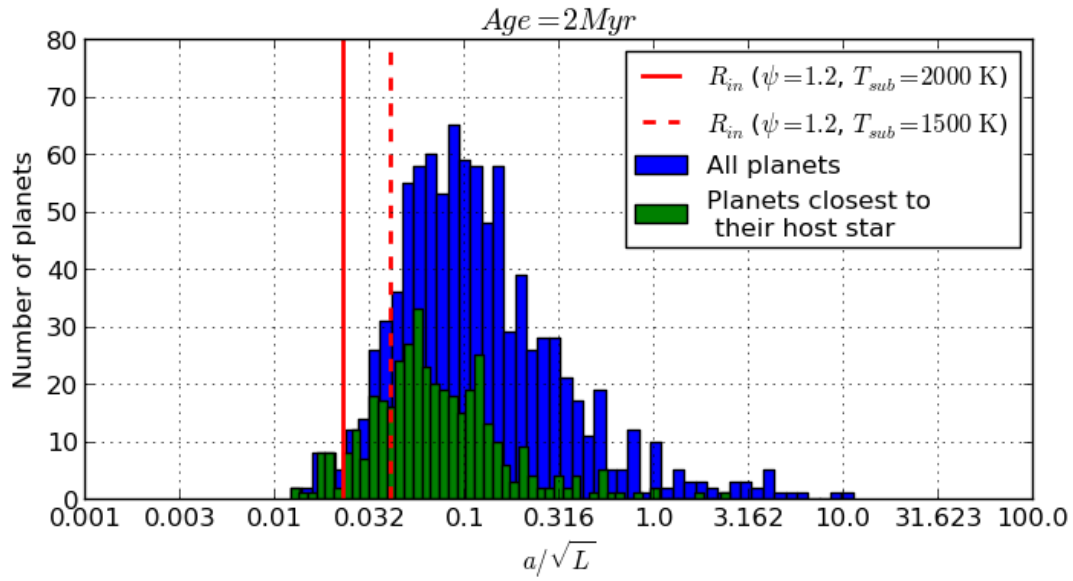


Figure 4.3: Number of planets with respect to semi-major axis (scaled by division by luminosity of the host star) at age 2 Myr

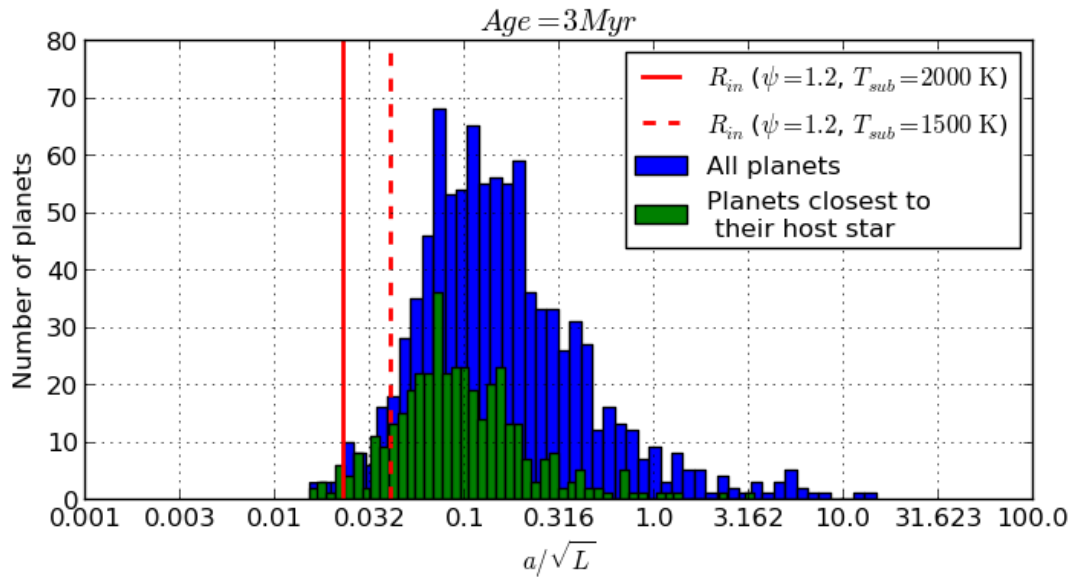


Figure 4.4: Number of planets with respect to semi-major axis (scaled by division by luminosity of the host star) at age 3 Myr

clustering and a cut-off near the inner radius can be seen⁵. Most of the planet formation seems to occur between 2 Myr and 3 Myr, the same conclusion as before.

⁵At first glance the distribution seems almost symmetric, but this is due to the usage of log scale. In reality, traversing the linearly scaled axis from left to right, one finds that there is a sharp increase in the density, and then a gradual decline

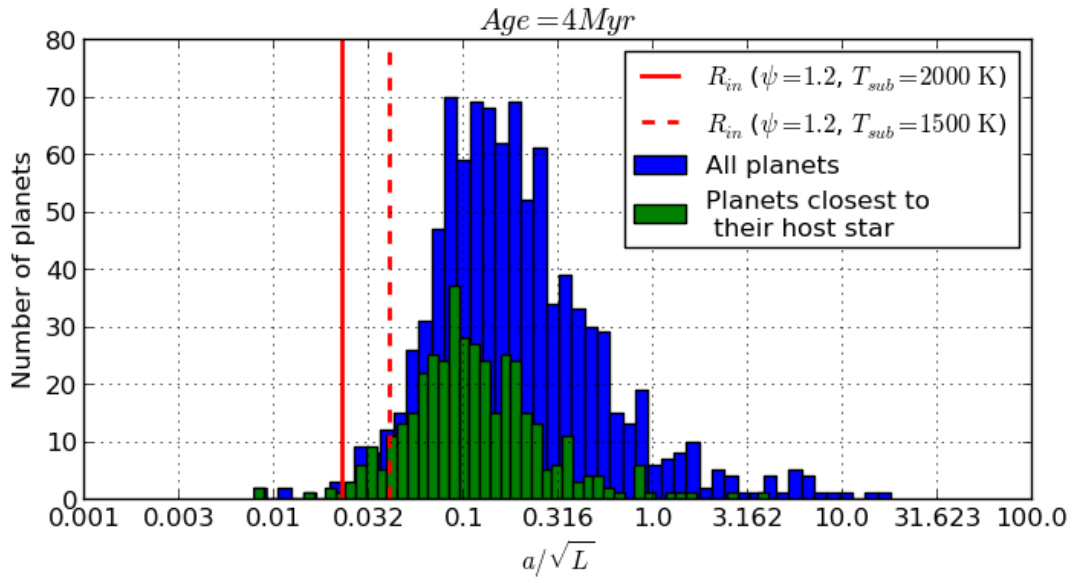


Figure 4.5: Number of planets with respect to semi-major axis (scaled by division by luminosity of the host star) at age 4 Myr

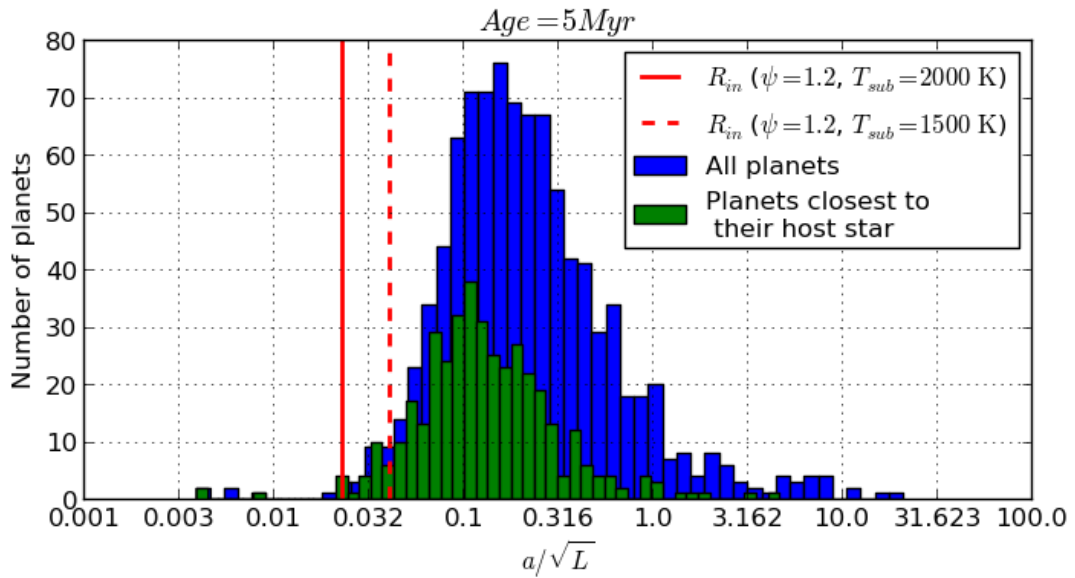


Figure 4.6: Number of planets with respect to semi-major axis (scaled by division by luminosity of the host star) at age 5 Myr

Chapter 5

Conclusion

It has been shown by others that a region devoid of dust exists in the center of protoplanetary disks, and surrounding it are dust sublimation zones, where some of the dust can exist in solid state. We hypothesised that planets should not be found in regions that were devoid of dust at the time of formation.

We searched the lists of detected extrasolar planets and compared those with the smallest semi major axis in their respective systems to the inner radii of the protoplanetary disks calculated for different ages between 1 Myr and 5 Myr. The inner radii are dependent on the luminosity of the star. The luminosities were obtained from the stellar evolution models, and are dependent on the age and the mass of the star. The fractions of planets closer than each of the inner radii were calculated.

The fractions of outliers were found to decrease during the age interval considered as a result of the increase of inner radii. Depending on the specific radius, the fractions of outliers at each age vary considerably, but those of the closest inner radii tend to be relatively small. The fractions of outliers are largest when considering only the Kepler Candidates and smallest when considering only confirmed planets.

The results were generally found to be compatible with the hypothesis, and suggesting that most of the planet formation happened around 2 Myr. However, due to small sample size, and many uncertainties, our results may not be representative of reality.

It was our aim to see if an analysis based on the inner radii and positions of planets relative to their host star can give support to either in situ formation of planets or theories of migration. As stated, no significant evidence of migration has been found, but the process of planet formation and migration is a debated issue, and it may not be as simple as represented here. For example, a two-phase model for hot super-Earths, starting with inward migration and followed by in situ phase, has been proposed (Raymond and Cossou, 2014).

Most of the detected planets were removed from the sample due to missing entries, and planet hunting is an ongoing process. For these reasons it would make sense to repeat this kind of analyses in the future, when more data is available. Interpretation of the results could be made more rigorous by focusing more on disk properties and distribution of planets at time of formation, and taking the details of different planet formation theories and new discoveries into account may prove to be illuminating in future analyses.

Appendix A

Python scripts

The python scripts that were used are given here. Note that, since the scripts rely on input files, running the scripts will result in an error message. The .zip file with the scripts and all the necessary files has been uploaded to www.pmfst.hr/~fralun/zavrsni/programski_dio.zip. The scripts were executed with the 2.7.3. version of Python interpreter (in order to run the scripts, numpy and matplotlib modules have to be installed). They should work with any newer 2.x version (probably with many older versions as well), but they can't be executed with versions 3.x.

filter.py

```
import csv
import pylab as pl
import numpy as np
import sys

tmin = 3000
tmax = 10000

def read(ime, firstline):
    cols = {}
    fl = open(ime, "r")
    data = csv.reader(fl)
    for line in data:
        if not data.line_num < firstline:
            if data.line_num == firstline:
                headers = line
                for h in headers:
                    cols[h] = []
            else:
                for h,v in zip(headers, line):
                    cols[h].append(v)

    fl.close()
    return cols

def write(ime, original, cols, firstline):
    fo = open(original, "r")
    rd = csv.reader(fo)
    dscr = []
    keys = []
    for line in rd:
        if rd.line_num < firstline:
            dscr.append(line)
        if rd.line_num == firstline:
            headers = line
```

```

        for h in headers:
            keys.append(h)
fo.close()

f1 = open(ime,"w")
wrt = csv.writer(f1)
lst = []
for k in keys:
    l = cols[k][:]
    l.insert(0,k)
    lst.append(l)
lst = zip(*lst)

for i in range(len(dscr)):
    wrt.writerow(dscr[i])
for i in range(len(lst)):
    wrt.writerow(lst[i])

f1.close()

#####

def Vece( (s1,plnum1), (s2,plnum2) ):
    if s1 > s2:
        return True
    if s1 == s2:
        if(float(plnum1) > float(plnum2)):
            return True
    return False

def Sort(cols, key1, key2):
    for i in xrange(len(cols[key1])):
        minind = i
        for j in xrange(i + 1, len(cols[key1])):
            if Vece( (cols[key1][minind], cols[key2][minind]), (cols[key1][j], cols[key2][j]) ):
                minind = j
        if minind != i:
            for k in cols.keys():
                temp = cols[k][i]
                cols[k][i] = cols[k][minind]
                cols[k][minind] = temp

#####

def Missing(cols, masskey, tempkey, smakey):
    missing = []
    for n in xrange( len( cols[masskey] ) ):
        if cols[masskey][n] == "":
            missing.append(True)
            continue
        if cols[tempkey][n] == "":
            missing.append(True)
            continue
        if cols[smakey][n] == "":
            missing.append(True)
            continue
    missing.append(False)

    return missing

def RemoveMissingData( cols, masskey, tempkey, smakey):

```

```

missing = Missing(cols , masskey , tempkey , smakey)
for key in cols.keys():
    cols[key] = [ item for n,item in enumerate(cols[key]) if not
                 missing[n] ]

#####

def Count(cols ,n,name,key):
    if (n+1) < len( cols[key] ):
        if cols[key][n+1] == name:
            return True
    if n>0:
        if cols[key][n-1] == name:
            return True
    return False

def Disp(cols):
    exterminate = []
    for n in xrange( len( cols["koi_disposition"] ) ):
        if cols["koi_disposition"][n] != "CANDIDATE":
            exterminate.append(True)
            continue
        if cols["koi_pdisposition"][n] != "CANDIDATE":
            exterminate.append(True)
            continue
        exterminate.append(False)

    for key in cols.keys():
        cols[key] = [ item for n,item in enumerate(cols[key]) if not
                    exterminate[n] ]

def Exterminate(cols ,namekey , masskey , tempkey , smakey , dispkey=""):
    exterminate = []
    for n in xrange( len( cols[namekey] ) ):
        plnumOK = Count(cols ,n,cols[namekey][n],namekey)
        if not plnumOK:
            exterminate.append(True)
            continue
        if not ( float(cols[tempkey][n]) > tmin
                and float(cols[tempkey][n]) < tmax):
            exterminate.append(True)
            continue

        exterminate.append(False)

    return exterminate

def Filter(cols ,namekey , masskey , tempkey , smakey , disp=""):
    exterminate = Exterminate( cols ,namekey , masskey , tempkey , smakey , disp )
    for key in cols.keys():
        cols[key] = [ item for n,item in enumerate(cols[key]) if not
                    exterminate[n] ]

##### MAIN #####

cols1 = read("ConfirmedPlanets2.csv",320)
cols2 = read("KeplerPlanetCandidates2.csv",142)

RemoveMissingData(cols1 , "st_mass" , "st_teff" , "pl_orbsmax")
RemoveMissingData(cols2 , "koi_smass" , "koi_steff" , "koi_sma")

Disp(cols2)

```

```

Sort(cols1,"pl_hostname","pl_orbsmax")
Sort(cols2,"kepid","koi_sma")

Filter(cols1,"pl_hostname","st_mass","st_teff","pl_orbsmax")
Filter(cols2,"kepid","koi_smass","koi_steff","koi_sma",disp="koi_disposition")

write("confirmed.csv","ConfirmedPlanets2.csv",cols1,320)
write("kepler.csv","KeplerPlanetCandidates2.csv",cols2,142)

```

"plot.py" can be run with or without a command line argument. If *i* is an integer, running as "plot.py *i*" will multiply the age parameter by *i*. After running the script, figures can be seen by entering "pl.show()".

plot.py

```

import csv
import pylab as pl
import numpy as np
import math
import sys
import os

def read(ime, firstline):
    cols = {}
    fl = open(ime, "r")
    data = csv.reader(fl)

    for line in data:
        if not data.line_num < firstline:
            if data.line_num == firstline:
                headers = line
                for h in headers:
                    cols[h] = []
            else:
                for h,v in zip(headers, line):
                    cols[h].append(v)

    fl.close()
    return cols

#####

def Prvi(cols, hostkey, n):
    if n == 0:
        return True
    if cols[hostkey][n] != cols[hostkey][n-1]:
        return True
    return False

#####

def Rsub(psi, Tsub, L):
    r = 0.0344 * psi * pow(1500.0 / Tsub, 2) * np.power(L, 0.5)
    return r

#####

```

```

def LinInterp(dX,dY,dx):
    k = dY / dX
    return k * dx

def LumsAux(name, age):
    name = round(name * 100)
    name = str( int( name ) ).zfill(3)
    name = "m" + name + "fehp00afem2.trk"

    model = np.loadtxt( os.path.join("fehp00afem2", name) )

    j = 0
    while model[j,0] < age:
        j += 1
    if model[j,0] == age:
        return model[j,3]
    else:
        interp = model[j-1,3] + LinInterp( model[j,0] - model[j-1,0], model
            [j,3] - model[j-1,3], age - model[j-1,0] )
        return interp

def Lums(m, age):
    lums = []
    listdir = [ ( float(item[1:4]) / 100 ) for item in os.listdir("fehp00afem2"
        ) ]
    listdir = sorted(listdir)

    for i in xrange( len(m) ):
        j = 0
        mass = round(m[i], 2)
        while listdir[j] < mass:
            j += 1
        if listdir[j] == mass:
            lums.append( LumsAux(listdir[j], age) )
        else:
            L1 = LumsAux(listdir[j-1], age)
            L2 = LumsAux(listdir[j], age)
            dl = L2 - L1
            dm = listdir[j] - listdir[j-1]
            interp = L1 + LinInterp( dm, dl, m[i] - listdir[j-1])
            lums.append(interp)

    return np.power(10.0, lums)

#####

def Manje(lums, plsma, psi, Tsub, age):
    r = np.log10( Rsub(psi, Tsub, lums) )
    manje = plsma < r
    return manje

###

def brManjih(aConf, lConf, aKOI, lKOI, psi, Tsub, age, LaTeX=False):
    manje = Manje(lConf, aConf, psi, Tsub, age)
    n = len( manje[manje == True] )
    if not LaTeX:
        print "\npsi=%s, Tsub=%d, age=%0.0f Myr" %(str(psi), Tsub, age/1e6)
        print ( "Za_confirmed: %d od %d (%.2f%%)" %(n, len(mConf), ( float(
            n)/len(mConf) ) * 100) )
    else:

```

```

prtstr = ( "%.0f\t&\t%s\t&\t%d\t&\t%d\t&%.2f\\%%\t&"%(age/1e6, str(
    psi), Tsub, n, ( float(n)/len(mConf) ) * 100) )

manje = Manje(lKOI, aKOI, psi, Tsub, age)
n = len( manje[manje == True] )
if not LaTeX:
    print ( "Za_candidates:_%d_od_%d_(%.2f%%)"
            %(n, len(mKOI), ( float(n)/len(mKOI) ) *
              100) )
else:
    prtstr += "\t%d\t&%.2f\\%%\t\\\\" %(n,( float(n)/len(mKOI) ) * 100)
    print prtstr

#####

def Plot(mRange, lums, psi, Tsub, line):
    Rin = np.log10( Rsub( psi, Tsub, lums ) )
    lbl = "$\psi_{sub} = %s, T_{sub} = %d \mathrm{K}$" %(str(psi), Tsub)
    pl.figure(1)
    pl.plot(mRange, Rin, line, label=lbl)
    pl.figure(2)
    pl.plot(mRange, Rin, line, label=lbl)

###

def CstFig(fignumber, mRange, aRange, age, legloc="lower_right"):
    pl.figure(fignumber)

    lbls = np.logspace(np.log10(0.001), np.log10(10), 5)
    tcks = np.log10( np.logspace(np.log10(0.001), np.log10(10), 5) )
    pl.yticks(tcks, lbls)

    pl.xlim(0, math.ceil(max(mRange)*2) / 2)
    pl.ylim(tcks[0], np.log10(math.ceil(pow(10,max(aRange)))))
    pl.title("$Age = %.0f \mathrm{Myr}$" % (age/1000000))
    pl.legend(loc=legloc)
    pl.grid()
    pl.xlabel("m_ [Msol]")
    pl.ylabel("a_ [AU]")

##### Keys #####

aConfKey = "pl_orbsmax"
aKOIKey = "koi_sma"
mConfKey = "st_mass"
mKOIKey = "koi_smass"
hostConfKey = "pl_hostname"
hostKOIKey = "kepid"

age = 1e6

##### MAIN #####

if len(sys.argv) > 1:
    age *= float(sys.argv[1])

cols1 = read("confirmed.csv",320)
cols2 = read("kepler.csv",142)

aConf = [ float(item) for n,item in enumerate( cols1[aConfKey] ) if Prvi(cols1,
    hostConfKey, n) ]

```

```

mConf = [ float(item) for n,item in enumerate( cols1[mConfKey] ) if Prvi(cols1,
    hostConfKey, n) ]
aKOI = [ float(item) for n,item in enumerate( cols2[aKOIKey] ) if Prvi(cols2,
    hostKOIKey, n) ]
mKOI = [ float(item) for n,item in enumerate( cols2[mKOIKey] ) if Prvi(cols2,
    hostKOIKey, n) ]
aConf = np.log10(aConf)
aKOI = np.log10(aKOI)

print "Confirmed:_" + str(len(aConf))
print "KOI:_" + str(len(aKOI))

massRange = np.linspace(0.1, 5, 200)
lums = Lums(massRange, age)

pl.figure(1, figsize=(8,4.5))
pl.clf()
pl.scatter(mKOI, aKOI, label="Kepler_Candidates")

pl.figure(2, figsize=(8,4.5))
pl.clf()
pl.scatter(mConf, aConf, label="Confirmed")

Plot(massRange, lums, 1.2, 2000, "r")
Plot(massRange, lums, 1.2, 1500, "r—")
Plot(massRange, lums, 2, 2000, "g")
Plot(massRange, lums, 2, 1500, "g—")

CstFig(1, mKOI, aKOI, age)
CstFig(2, mConf, aConf, age)

lConf = Lums(mConf, age)
lKOI = Lums(mKOI, age)
LaTeX = False
brManjih(aConf, lConf, aKOI, lKOI, 2, 1500, age, LaTeX)
brManjih(aConf, lConf, aKOI, lKOI, 2, 2000, age, LaTeX)
brManjih(aConf, lConf, aKOI, lKOI, 1.2, 1500, age, LaTeX)
brManjih(aConf, lConf, aKOI, lKOI, 1.2, 2000, age, LaTeX)

```

Bibliography

Vinković, D. 2006, ApJ, 651, 906

Ribas, Á. et al. 2006, A&A, 561, A54

Rowe, J. F. et al. 2014, ApJ, 784, 45

Vinković, D. and Jurkić, T. 2007, ApJ; 658; 452

Raymond, S.N. and Cossou, C. 2014, MNRAS, 440, L11

Dotter, A. et al. 2007, AJ, 134, 376

Armitage, P.J. 2007, Lecture notes on the formation and early evolution of planetary systems
[arXiv:astro-ph/0701485]